The 2025 World Congress on
Advances in Structural Engineering and Mechanics (ASEM25)
BEXCO, Busan, Korea, August 11-14, 2025

Methodology for Assessing Uncertainty in Joint Roughness Considering Measurement Accuracy and Spatial Distribution

Juhyi Yim[1)], Han-Byul Kang[2)], Jae-Hoon Jung[2)], and Young-Jin Shin[3)*]

[1), 2), 3)]R&D Center, Hyundai Construction and Engineering, Seoul, Korea
[3)] johnyj.shin@hdec.co.kr*

ABSTRACT

Joint Roughness Coefficient (JRC) is a critical parameter for evaluating the shear strength of rock joint surfaces, but accurately determining it in the field remains challenging due to inherent measurement error in both traditional 2D profiling and modern 3D scanning methods. Thus, reliable characterization of joint roughness requires methodologies that explicitly account for this error in field-acquired data. This study presents a method to assess the spatial distribution of JRC on a joint surface by analyzing multiple profiles and to quantify the uncertainty in roughness by incorporating measurement error. Multiple profiles extracted from LiDAR scans of a single rock joint are evaluated for roughness using the Z_2 index, a 3D metric correlated with JRC. A statistical approach then integrates the measurement error associated with 3D scanning to estimate confidence intervals for the computed JRC values. Results demonstrate that the proposed approach significantly reduces bias in JRC estimation and improves the consistency of roughness measurements. These findings enable more efficient and robust characterization of joint surfaces, supporting the design and construction of large-scale underground structures such as deep geological repositories for spent nuclear fuel.

1. INTRODUCTION

Accurate assessment of joint shear strength is essential for the design and stability of underground structures such as large caverns and deep geological repositories. Among the governing parameters, joint roughness plays a significant role in determining shear resistance. The Joint Roughness Coefficient (JRC), proposed as an empirical index, represents this surface roughness and is traditionally determined by comparing measured 2D joint profiles to standard reference charts using tools such as the Barton comb (Barton and Choubey, 1977).

[1)] Researcher
[2)] Senior Researcher
[3)] Senior Researcher

To reduce subjectivity in JRC estimation, various quantitative indices such as the structure function (Z_2) and tilt angle (θ) have been proposed. These indices have been correlated with JRC through empirical models (Tatone and Grasselli, 2012; Huang et al., 2019). With the advancement of 3D scanning technologies, several attempts have been made to derive these indices directly from three-dimensional joint surface data (Grasselli, 2001; Khoshelham et al., 2011; Ge et al., 2021). However, such studies have predominantly relied on laboratory setups or required high-precision instruments that are impractical for routine field applications.

In field conditions, 3D scanning data often include inherent measurement errors due to limitations in device resolution, scanning distance, and surface reflectivity. These errors can obscure true joint roughness and lead to unreliable JRC estimates. Figure 1 illustrates the difference in resolution between laboratory-scale and field-scale scanning data of joint surfaces, highlighting the potential distortion introduced by field-acquired measurements.

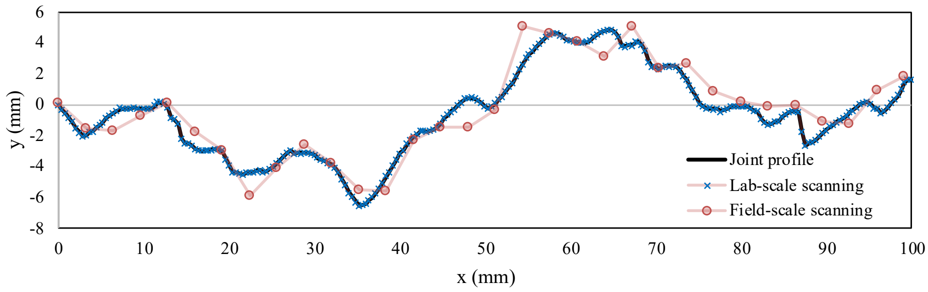

Fig. 1 Simulated lab-scale and field-scale scanning data of the joint profile (Grasselli, 2001).

This study proposes a methodology for quantifying the uncertainty of JRC derived from field-based 3D scanning data. The approach involves evaluating the Z_2 index from LiDAR-acquired joint profiles and converting it into JRC using an established empirical relation. The effect of measurement error and spatial variability is incorporated into a statistical framework to derive confidence intervals for the estimated JRC. This method facilitates reliable roughness assessment using practical 3D scanning techniques and supports automated geotechnical classification systems such as RMR. While the detailed effect of roughness on joint shear strength is a critical topic in rock mechanics, it is beyond the scope of the present paper.

2. THEORETICAL BACKGROUND

Let the X-axis denote the direction of the joint profile and the XY-plane represent the best-fitting plane of the joint surface. Each profile consists of M points equally spaced by ΔX, and a total of N profiles are extracted from the surface. The roughness index Z_2 for a 2D profile and its extension to a representative 3D surface value are defined as follows in Eq. (1) and Eq. (2) (Ge et al., 2021). Z_0 denotes the random variable representing the z-values at each point on the joint surface, Z_{+1} represents the random variable of the z-values at adjacent points to Z_0, and V refers to a function that computes the variance of a given random variable.

$$Z_{2,2D}^2 = \frac{1}{\Delta X^2}\frac{1}{M-1}\sum_{M-1}(z_{i+1}-z_i)^2 = \frac{1}{\Delta X^2}V(Z_{+1}-Z_0) \tag{1}$$

$$Z_{2,3D}^2 = \frac{1}{N}\sum_{N} Z_{2,2D}^2 \tag{2}$$

let the random variable of measurement error be denoted by E, and let measured properties that include this error be indicated with the subscript m. Then, the random variable of the measured z-values is denoted by Z_m. Since each of these variables is independent, Eq. (3) holds.

$$V(Z_{+1,m}-Z_{0,m}) = V(Z_{+1}+E_{+1}-Z_0-E_0) = V(Z_{+1}-Z_0)+V(E_{+1})+V(E_0) \tag{3}$$

Assuming the standard deviation of the measurement error is σ_E and it follows a normal distribution with zero variance, and the population variance is approximated by $Z_{2,3D}$, then Eqs. (4) and (5) hold for the squared Z_2 values of the profile. Here, $Z_{2,3D}$ represents the representative value of Z_2 in three-dimensional space, and σ^2_{3D} denotes the variance of a sample of size N for the squared $Z_{2,2D}$ values of the profile.

$$Z_{2,3D}^2 = E\left(Z_{2,2D,m}^2\right) - \frac{2\sigma_E^2}{\Delta X^2} \tag{4}$$

$$\sigma_{3D}^2 = \frac{V\left(Z_{2,2D}^2\right)}{\sqrt{N}} = \frac{V\left(Z_{2,2D,m}^2\right)}{\sqrt{N}} - \frac{1}{\sqrt{N}}\left(\frac{M-2}{M-1}\frac{1}{\Delta X^2}\right)^2\left(\frac{8}{M-2}\sigma_E^4\right) - \left(\frac{M-2}{M-1}\frac{1}{\Delta X^2}\right)^2\frac{8\Delta X^2}{M-1}Z_{2,3D}^2\sigma_E^2 \tag{5}$$

3. EXPERIMENT

3.1 Experimental setup

A field-scale experiment was conducted at a tunnel excavation site in granitic gneiss, where a representative tunnel face was scanned at four distances (3 m, 5 m, 7 m, and 10 m) using the Leica RTC360 LiDAR scanner. The scanner was operated at maximum resolution, corresponding to 3 mm accuracy at a 10 m distance. Each scan was completed within 2 minutes, producing point clouds of approximately 1.5 GB (about 4.1 million points).

To obtain a reference model, high-resolution 3D scanning of the target joint surface was conducted at close range using a SCANTECH KSCAN Magic laser scanner. The device provides a point spacing of 0.1 mm and accuracy of 0.01 mm. The high-resolution 3D scanned surface was treated as the reference case for comparison (Fig. 2).

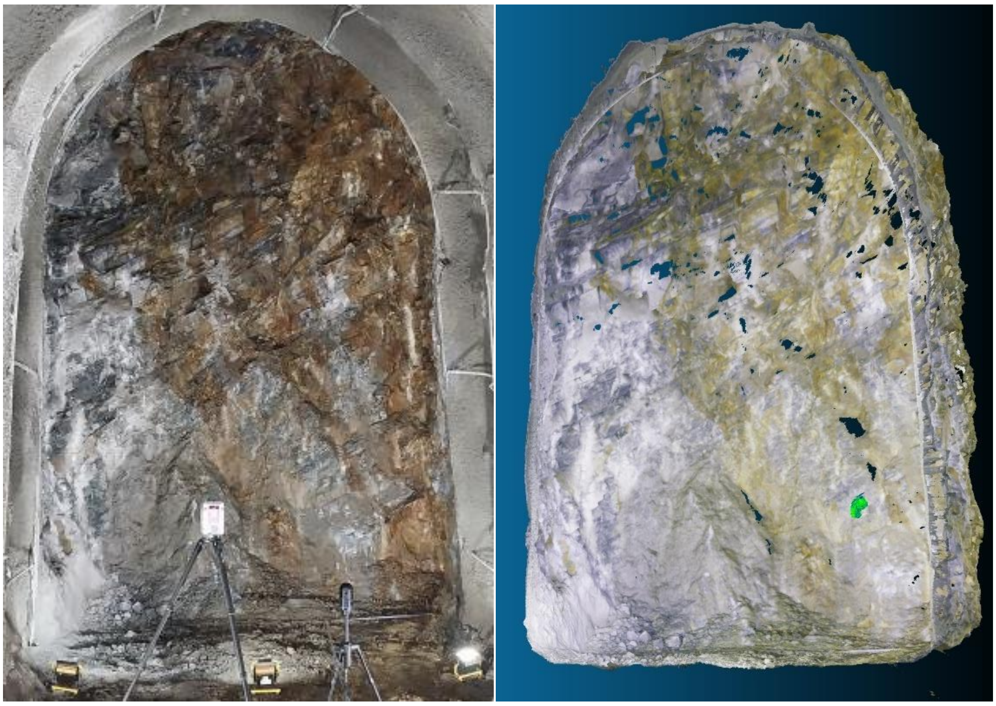

Fig. 2 (Left) Tunnel face with RTC360 LiDAR scanning, (Right) 3D model of tunnel face. Green area indicates the region scanned with high-precision laser scanning.

3.2 Joint roughness evaluation

The joint surface was extracted from the full point cloud and cropped to a rectangular region of interest. This subset was rotated so that its best-fitting plane aligned with the XY-plane. A grid was generated in the XY-plane using a spacing equal to the average point interval, and elevation (Z) values at each grid node were interpolated to construct a raster dataset (Fig. 3).

The roughness index Z_2 was computed from this raster. For each profile, JRC was estimated using the empirical Z_2–JRC relationship defined in Eq. (6), valid for sampling intervals between 0.1 mm and 5 mm (Huang et al., 2019).

$$JRC = -5.75\Delta x^{-0.41} + 70.28\,\Delta x^{0.09}\,Z_2 \tag{6}$$

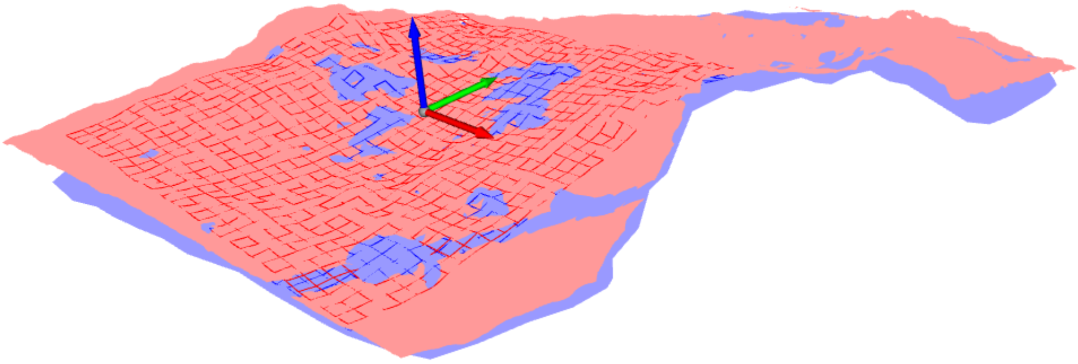

Fig. 3 Rasterized representation of the joint surface: (Red) Reference case, (Blue) LiDAR-measured case.

4. Result

To ensure a consistent comparison between reference and LiDAR datasets, the largest overlapping area of the joint surface was selected, measuring approximately 1000 mm × 820 mm. A uniform grid was applied in both the X and Y directions. To minimize the influence of localized anomalies, areas showing abrupt JRC variation were excluded, and two representative subregions were defined as Case A and Case B (Fig. 4).

Input parameters and computed results for each case are summarized in Table 1. The table includes sampling intervals, scanner accuracy (defined as the standard deviation of distance residuals; Bauer and Woschitz, 2024), number of profile points, number of profiles, squared Z_2, and corresponding JRC values. For each entry, measured values, reference values, and statistically corrected estimates are listed. Confidence intervals (90%) for the corrected JRC are also provided.

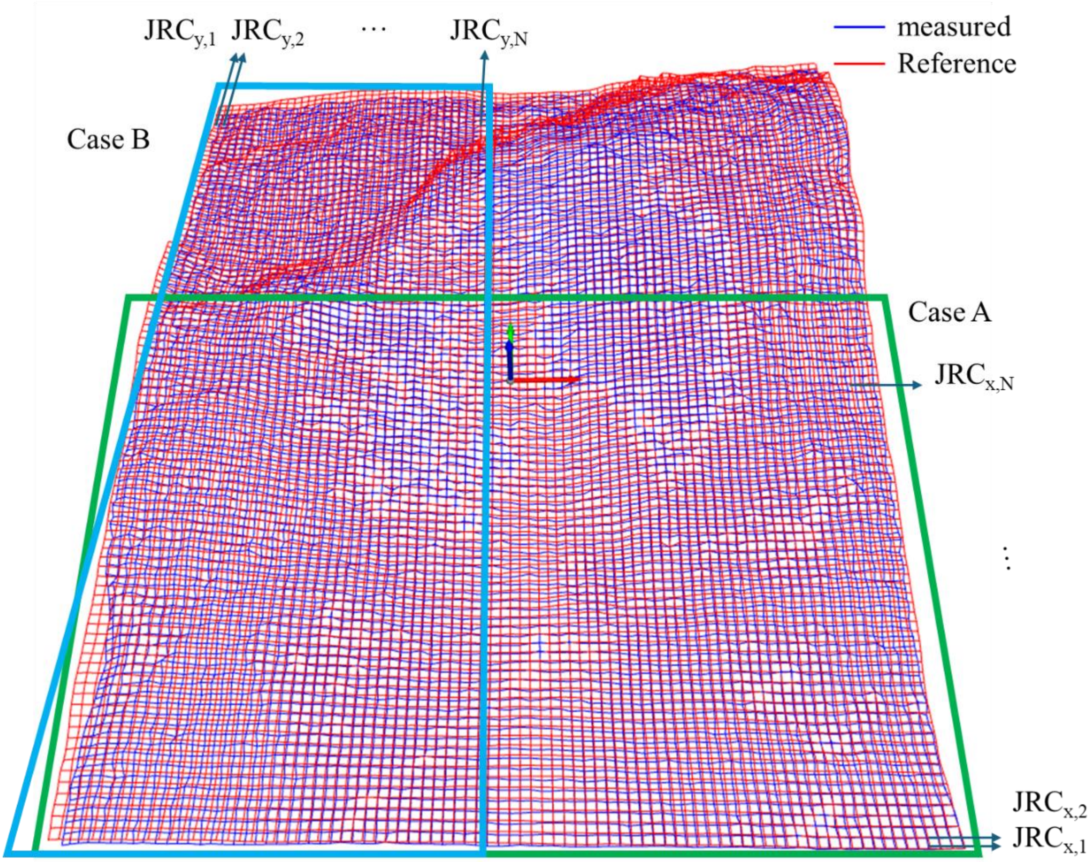

Fig. 4 Gridded joint surface showing the selected regions for Case A (X-directional profiles) and Case B (Y-directional profiles)

Table 1 Input parameters for Eqs. (4)-(6) and calculated joint roughness parameters the joint plane in Fig. 4. Parentheses indicate variation, while square brackets represent 90% confidence interval (*Bauer and Woschitz, 2024)

		Case A (x-directional joint profiles)				Case B (y-directional joint profiles)			
Sampling interval (mm)		1	1.41	1.99	2.82	1	1.41	1.99	2.82
Accuracy (mm)*		0.22	0.245	0.27	0.35	0.22	0.245	0.27	0.35
# of points in joint profile		83	59	42	30	101	72	51	36
# of joint profiles		59	40	29	21	28	20	15	10
Z_2^2	Measured	0.1357 (0.028)	0.0984 (0.0234)	0.0708 (0.0201)	0.0599 (0.0205)	0.147 (0.0242)	0.0999 (0.0213)	0.0793 (0.0183)	0.0581 (0.0074)
	Reference	0.0377 (0.0146)	0.0348 (0.0138)	0.0309 (0.0122)	0.0279 (0.0113)	0.0658 (0.0225)	0.0581 (0.017)	0.0506 (0.0124)	0.0438 (0.0077)
	Estimated	0.0389 (0.0194)	0.038 (0.0165)	0.0339 (0.015)	0.0291 (0.0155)	0.0502 (0.0145)	0.0396 (0.0148)	0.0425 (0.0128)	0.0273 (-)
JRC	Measured	20.1	17.7	15.6	15.1	21.2	17.9	16.7	14.8
	Reference	7.9	8.5	8.8	9.1	12.3	12.5	12.5	12.4

Confidence interval	[7.4,8.8]	[8.3,9.9]	[8.5,10.3]	[8.1,10.6]	[9.3,10.7]	[8.4,10.4]	[10.1,12]	[9.0]

As shown in Fig. 5, JRC values estimated directly from LiDAR data are significantly overestimated compared to the reference case due to the influence of measurement error. After applying the proposed correction methodology, the RMS difference in JRC was reduced from approximately 7.5 to 1.9. Similarly, for Z_2^2 variance, the RMS error was reduced from 0.0082 to 0.0042.

In the reference data, increasing the sampling interval resulted in a decrease in Z_2^2, as expected. However, the corresponding JRC values remained nearly constant due to the use of the empirically calibrated Z_2–JRC relation (Eq. 6), confirming that the influence of sampling resolution was appropriately compensated.

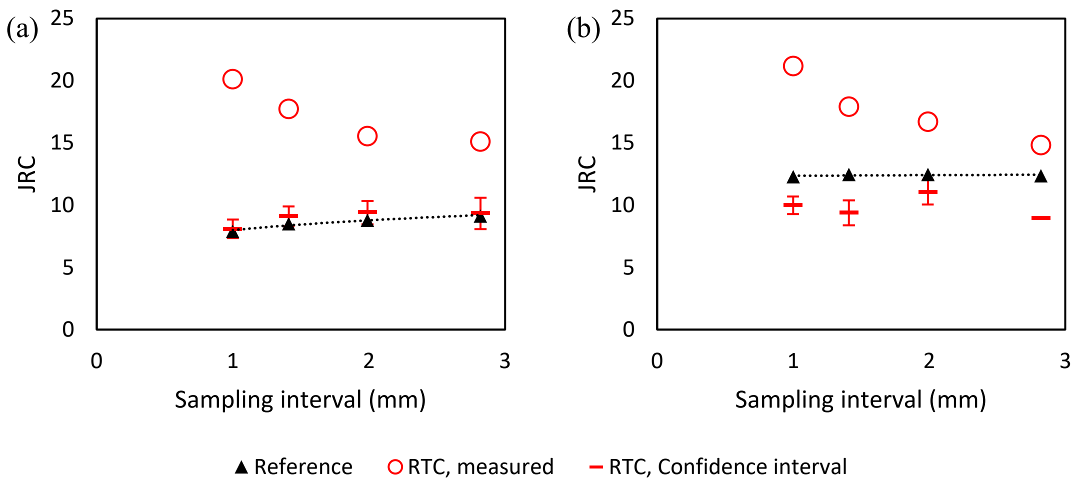

Fig. 5 Comparison of joint roughness coefficients for the reference case and RTC360-measured cases of (a) Case A (X-directional profiles) (b) Case B (Y-directional profiles)

5. Discussion

5.1 Joint roughness underestimation due to systematic error

Measurement error in LiDAR data can be broadly categorized into statistical (random) and systematic components. While random error increases apparent roughness and was addressed using the statistical correction presented in Section 2, systematic error—such as smoothing of sharp asperities—can cause underestimation of joint roughness.

Figure 6a shows the distribution of JRC values across the x-directional profiles in Case A. Most profiles exhibit JRC overestimation in the LiDAR-measured data compared to the reference, attributed to random noise (Fig. 6b). However, in locations with pronounced asperities, as shown in Fig. 6c, the LiDAR system tends to smooth these features due to limitations in laser resolution. This smoothing can lead to JRC values from LiDAR being lower than those from the reference scan, as illustrated in Fig. 7.

Across the entire surface, comparison of average JRC values from corrected LiDAR data and the reference scan indicates a consistent underestimation of approximately 5.4. This suggests that even after compensating for random error, residual bias remains due to uncorrected systematic effects. Addressing such bias requires further investigation into the interaction between surface morphology and scanning resolution, potentially involving model-based compensation or hybrid scanning strategies.

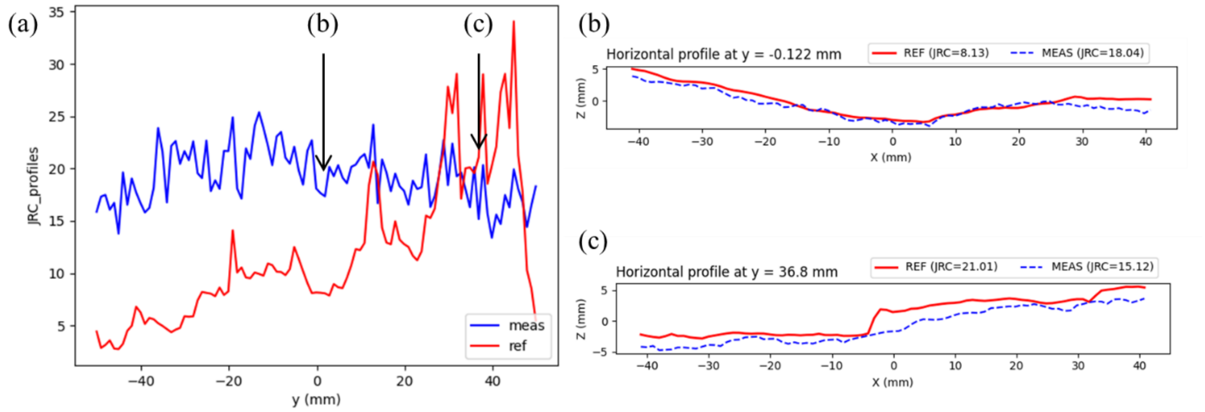

Fig. 6 (a) Joint roughness coefficient distribution of x-directional joint profiles and x-directional joint profiles of reference and RTC360-measured case at (b) y=-0.122mm and (c) y=36.8mm (LiDAR at 3 m)

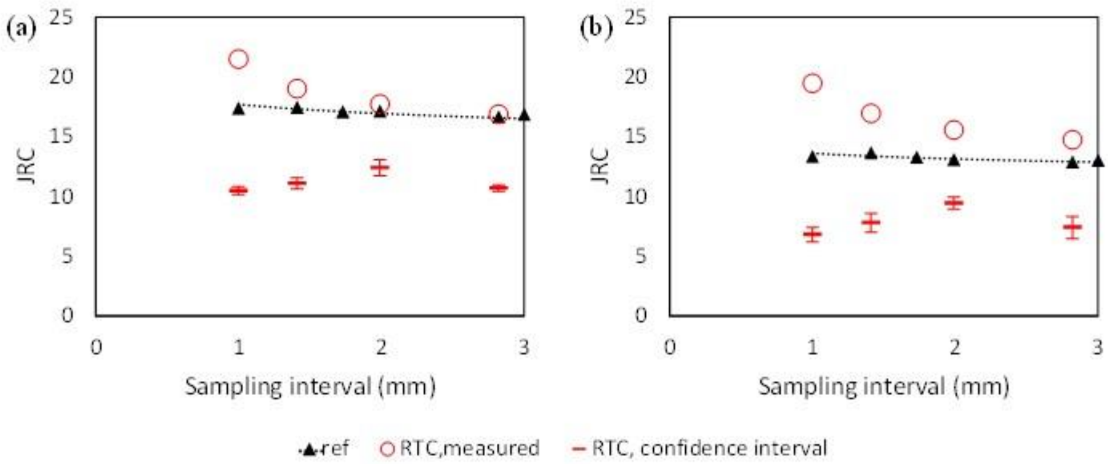

Fig. 7 Comparison of joint roughness coefficients for the reference case and RTC360-measured cases of (a) x-directional joint profiles and (b) y-directional joint profiles over the full joint plane in Fig. 4.

5.2 Field applicability and Operational Constraints

Field applicability of the proposed method depends on the resolution and accuracy achievable under practical scanning conditions. For the Leica RTC360, scanner-to-face distance (d) typically ranges from 3 m to 20 m. The resulting sampling interval (Δx) is governed by distance and scanner resolution, and accuracy (σ_E) is influenced by surface reflectivity and incident angle (Bauer and Woschitz, 2024).

$$\Delta x\ (mm) = 0.3\ d\ (m) \tag{7}$$

According to Ge et al. (2021), the minimum required resolution to capture joint morphology is a function of the sampling size L, i.e., the spatial extent of the joint patch. This relationship can be expressed as (Eq. (8)):

$$\Delta x\ (mm) = \begin{cases} 0.015\ L(mm)\ (Rough\ joint) \\ 0.030\ L(mm)(Smooth\ joint) \end{cases} \tag{8}$$

Table 2 presents typical field scanning conditions. When the exposed joint surface exceeds 300 mm × 300 mm, reliable JRC estimation is achievable even at a 15 m scanning distance, assuming systematic error is negligible or can be filtered. If smoothing effects are non-negligible, localized high-resolution scans or empirical correction factors may be required.

Table 2 Operational Constraints and Conditions of LiDAR in Field (RTC360).

Distance from tunnel face, d (m)	Sampling interval, Δx (mm)	Sampling size, L (mm)	Accuracy, σ_E (mm)
3	0.9	60 (rough)	0.22
15	4.5	300 (rough)	0.55

These results indicate that LiDAR-based roughness assessment is feasible for large-scale joint exposures commonly encountered in tunnel construction. Integration of error correction and surface filtering allows for robust in-situ JRC estimation under realistic conditions.

6. Conclusion

This study proposed a method for estimating joint roughness coefficients (JRC) from field-acquired 3D scanning data, incorporating both measurement error and spatial variability into the evaluation process. Application to a tunnel face in granitic gneiss demonstrated the method's effectiveness under realistic field conditions.

Key findings are summarized as follows:

- Direct JRC estimation from uncorrected LiDAR data resulted in significant overestimation, with an average deviation of up to 12.2. Applying a statistical correction reduced this deviation to approximately 1.9.

- In regions with large local asperities, systematic smoothing effects inherent to the LiDAR caused underestimation of JRC, even after correcting for random error.

This led to an average underestimation of approximately 5.4 compared to the high-precision reference.

- The proposed method enables estimation of not only average JRC values but also confidence intervals, thereby quantifying uncertainty due to measurement error and inherent spatial variation.
- Field applicability was demonstrated by defining operational constraints. Reliable JRC estimation is feasible at scanning distances up to 15 m when surface exposure exceeds 300 mm, provided that systematic error is minimal or appropriately addressed.

The presented approach provides a practical and statistically sound framework for in-situ joint roughness evaluation using terrestrial LiDAR. The methodology supports integration into rock mass classification and automated geotechnical assessment workflows for underground construction.

ACKNOWLEDGMENTS
This work was supported by the Institute for Korea Spent Nuclear Fuel (iKSNF) and Korea Institute of Energy Technology Evaluation and Planning (KETEP) grant funded by the Korea government (Ministry of Trade, Industry and Energy, MOTIE) (No. RS-2023-KP002657)

REFERENCES

Barton, N., & Choubey, V. (1977). *“The shear strength of rock joints in theory and practice.”* Rock Mechanics, **10**(1–2), 1–54.

Bauer, P., & Woschitz, H. (2024). *“Laboratory Investigations of the Leica RTC360 Laser Scanner—Distance Measuring Performance.”* Sensors, **24**(12), 3742.

Ge, Y., Lin, Z., Tang, H., & Zhao, B. (2021). *“Estimation of the appropriate sampling interval for rock joints roughness using laser scanning.”* Bulletin of Engineering Geology and the Environment, **80**(5), 3569–3588.

Grasselli, G. (2001). *“Shear strength of rock joints based on quantified surface description.”* Ph.D. thesis, École Polytechnique Fédérale de Lausanne (EPFL), Switzerland.

Huang, M., Xia, C., Sha, P., Ma, C., & Du, S. (2019). *“Correlation between the Joint Roughness Coefficient and rock joint statistical parameters at different sampling intervals.”* Advances in Civil Engineering, **2019**, Article ID 1643842.

Khoshelham, K., Altundag, D., Ngan-Tillard, D., & Menenti, M. (2011). *“Influence of range measurement noise on roughness characterization of rock surfaces using terrestrial laser scanning.”* International Journal of Rock Mechanics and Mining Sciences, **48**(8), 1215–1223.

Tatone, B. S. A., & Grasselli, G. (2012). *“An investigation of discontinuity roughness scale dependency using high-resolution surface measurements.”* Rock Mechanics and Rock Engineering, **45**(3), 619–645.